Revisiting Thin-Layer Electrochemistry in a Chip-Type Cell for the Study of Electroorganic Reactions

Samuel J. Shin,[‡1] Ji Yong Kim,[‡1] Sohee An,[1] Moonjoo Kim,[1] Minjee Seo,[2] Su Yong Go,[1] Hyunho Chung,[1] MinKeun Lee,[1] Min-Gyeong Kim,[3] Hong Geun Lee,[1] Taek Dong Chung*[1,4]

[1]Department of Chemistry, Seoul National University, Seoul, 08826, Republic of Korea

[2]Department of Chemistry Education, Korea National University of Education, Cheongju-si, Chungbuk 28173, Republic of Korea

[3]Department of Chemistry Education, Seoul National University, Seoul, 08826, Republic of Korea

[4]Advanced Institutes of Convergence Technology, Suwon-si, Gyeonggi-do, 16229, Republic of Korea

‡ These authors contributed equally.

ABSTRACT: It is important but challenging to elucidate the electrochemical reaction mechanisms of organic compounds using electroanalytical methods. Particularly, a rapid and straightforward method may be helpful if it can provide information on reaction intermediates or other key electrochemical parameters. In this work, we exploited the advantages of classic thin-layer electrochemistry to develop a thin-layer electroanalysis microchip (TEAM). TEAM provided better resolved voltammetric peaks than under semi-infinite diffusion condition owing to the small height. Importantly, rapid and accurate determination of the number of electrons transferred, *n*, was enabled by mechanically confining the microliter-scale volume analyte at the electrode, while securing ionic conduction using polyelectrolyte gels. The performance of the TEAM was validated using voltammetry and coulometry of standard redox couples. Utilizing TEAM, a (spectro)electrochemical analysis of FM 1-43, an organic dye widely used in neuroscience, was successfully performed. It was also applied to study the electrochemical oxidation mechanism of pivanilides and alkyltrifluoroborate salts with different substituents and solvents. This work suggests the TEAM as a promising tool to provide invaluable mechanistic information and promote the rational design of electrosynthetic strategies.

KEY WORDS: thin-layer electrochemistry, thin-layer electroanalytical chip, electrochemical oxidation mechanism, number of electrons, voltammetry, coulometry, spectroelectrochemistry, FM 1-43, pivanilides, alkyltrifluoroborate salts, electroorganic chemistry

INTRODUCTION

Understanding the mechanisms of electrochemical reactions is important for rationally utilizing/producing molecules for use in the fields of energy/chemical conversions,[1–4] bioelectrochemistry,[5] and organic electrosynthesis.[6–11] It is especially critical in synthetic organic electrochemistry to improve yields or control reaction selectivity among competing pathways.[12,13] However, heterogeneous electrochemical reactions are challenging to understand because electrochemically measured information of current or potential hardly provides chemical information about species under electrochemical reaction. For example, the nature of reaction intermediates, e.g., free radicals, radical ions, ions, often cannot be predicted by electrochemical analysis and requires various control experiments of synthetic scale,[10,14–16] DFT and *ab initio* calculations,[17,18] or spectroscopic measurement such as electron paramagnetic resonance spectroscopy.[15] Therefore, there are extensive needs for straightforward electroanalytical methods to provide evidences on reaction intermediates and the key parameters which would unveil electrochemical reaction mechanisms. Yet, limited efforts have been made to develop suitable electrochemical techniques for such purpose.[12,13,19,20]

Among the electroanalytical methods, cyclic voltammetry has been the most widely used technique in mechanistic studies for decades. The number of voltammetric peaks, reversibility, relative peak currents, or peak potential shift provides basic information on the electrochemical reaction. Square wave voltammetry has recently gained attention to distinguish multi-electron transfers underneath an apparently single peak of cyclic voltammogram in specific cases.[14,21] Nevertheless, generalization of these methods requires further improvements, such as enhancing the peak resolution. A more intuitive and critical knowledge of reaction pathway is the number of electrons transferred per molecule in a heterogeneous redox reaction, n. For instance, knowing n helps infer electrogenerated reaction intermediates, e.g., a radical resulting from one-electron transfer, an (radical) ion resulting from the two-electron transfer. In fact, electrochemical methods such as hydrodynamic methods using rotating disk electrode,[22,23] or chronoamperometric techniques using macro or microelectrode[24,25] have been utilized for such purpose. However, these are not applicable to complicated systems of multiple electron transfer and chemical reaction steps, and even are troublesome to be conducted in nonaqueous systems with low viscosity.[26]

Thin-layer electrochemistry at which reactants reside within <30 μm from the electrode has been investigated since the 1960s. Owing to its mathematical simplicity and unique voltammetric features in the absence of semi-infinite inbound mass transfer, thin-layer electrochemistry has been exploited to estimate kinetic parameters for sluggish reactions[27,28] or adsorption reactions and to determine diffusion coefficient or stoichiometry.[29,30] Furthermore, spectroelectrochemical studies in thin-layer cells using grid electrodes or transparent electrodes could benefit from low background signal.[31,32] Despite numerous theoretical demonstrations on its usefulness, thin-layer electrochemistry has been impeded by lateral diffusion from the external solution and the absence of a standardized system.

By revisiting thin-layer electrochemistry, we devised a microchip device, a thin-layer electroanalysis microchip (TEAM), to extract more information about the electrochemical reaction mechanism. Both computational simulations and experimental results show that the voltammetric response from the thin-layer cell can give better resolved neighboring peaks. More importantly, lateral diffusion was prevented by mechanically confining the micro-volume analyte solution to the working electrode using a polyelectrolyte gel salt bridge, thus enabling accurate determination of n via electrolysis. A lipophilic polyelectrolyte gel was introduced to allow the TEAM to operate in various organic solvents as well as an aqueous solution. Based on such development, the TEAM could be used as a versatile tool to study various electrochemical organic reactions. In addition, TEAM could also be utilized as a spectroelectrochemical cell by using a transparent electrode of indium tin oxide (ITO) as the working electrode. This work demonstrates the TEAM as a straightforward electroanalytical device for exploring electrochemical reaction mechanism.

RESULTS AND DISCUSSION

Digital simulation. The thin-layer electrochemical characteristics of the TEAM are expected to offer better distinguishable voltammetric peaks in multi-step electron transfer reactions. Digital simulation of square wave voltammetry was performed to verify this feature under thin-layer of 20 μm compared to that under semi-infinite diffusion condition for the model system of two sequential oxidation reactions as follows.

$$R \rightleftharpoons O + e^- \quad (E_1^0, k_1^0) \qquad (1)$$

$$O \rightleftharpoons O' + e^- \quad (E_2^0, k_2^0) \qquad (2)$$

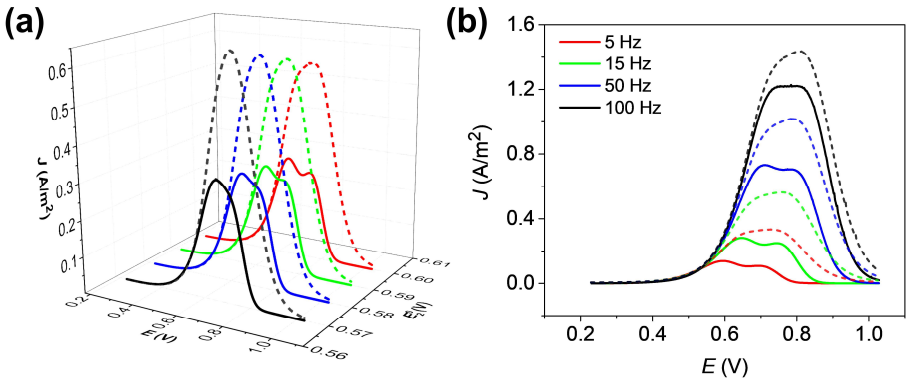

Figure 1. Simulated SWV curves of thin-layer cell of 20 μm (solid line) and semi-infinite diffusion model (dashed line) at different (a) ΔE^0 and (b) frequency. Step potential and amplitude were set as 2 mV and 15 mV each, diffusion coefficients were 5×10^{-6} cm^2/s for all the species, k_1^0=0.00015 cm/s, k_2^0=0.0001 cm/s, and E_1^0 was 0.5 V. Frequency was 15 Hz for (a) and E_2^0 was 0.6 V for (b).

Figure 1a demonstrates the effect of $\Delta E^0, E_2^0 - E_1^0$, on square wave voltammogram (SWV) peak shape obtained by varying redox potential of second oxidation (E_2^0). The resulting two neighboring peaks are more distinguishable in the thin-layer cell than under semi-infinite diffusion conditions for the same ΔE^0. This superior resolution of voltammetry in thin-layer cell stems from the difference in diffusion behavior. With solution thickness smaller than diffusion layer thickness, the concentration profile of redox species throughout the entire cell changes with electrode potential (Video S1), reducing the mass transfer effect. As a result, earlier peak potential appears with steeper current decrease due to the fast depletion of reactants without semi-infinite inbound diffusion (Figure S1). Meanwhile, SWVs as a function of frequency indicate that the peak separation is more evident at lower frequencies than at higher frequencies (Figure 1b). A low frequency is favorable for observing such distinctive thin-layer electrochemistry behavior because a longer experiment duration is beneficial to achieve mass transfer equilibrium throughout the cell. This observed frequency effect caused by limited diffusion length shows the opposite trend to that observed in the previous report, which was originated from the kinetics aspect.[21]

Design of the TEAM and validation of its performance. To enable investigation of an electrochemical reaction by thin-layer voltammetry and small volume electrolysis, the TEAM was devised (Scheme 1). Briefly, it is composed of three parts: the analysis chamber with the working electrode, a channel encompassing the chamber where the reference and the counter electrodes are placed, and the polyelectrolyte gel salt bridge formed between the chamber and the channel. The small height of 20 μm allows immediate access of reactants to the electrode surface while also imparting the characteristic voltammetric features of thin-layer cells. Most importantly, lateral diffusion was prevented by mechanically confining the microliter-scale volume analyte solution to the chamber using a polyelectrolyte gel salt bridge. This enabled the accurate determination of *n* via coulometry in a short time. For analysis in aqueous solutions, polydiallyldimethylammonium chloride (pDADMAC) hydrogel[33] was constructed in the TEAM. However, pDADMAC collapsed in organic solutions because of ion aggregation in low polarity solvents (Figure S2a). To tackle this problem, a photopolymerizable lipophilic polyelectrolyte gel with

hydrophobic backbone and anion was developed based on previous studies and introduced into the TEAM.[34,35] Thus introduced polylaurylacrylate tetrakis[3,5-bis(trifluoromethyl)phenylborate (pLA-TFPB) (Scheme 2) successfully worked as a salt bridge in organic solvents tested (Figure S2b).

SCHEME 1. Schematic representations of TEAM. (a) The overall structure and (b) cross-sectional view (left and top view (right) of TEAM.

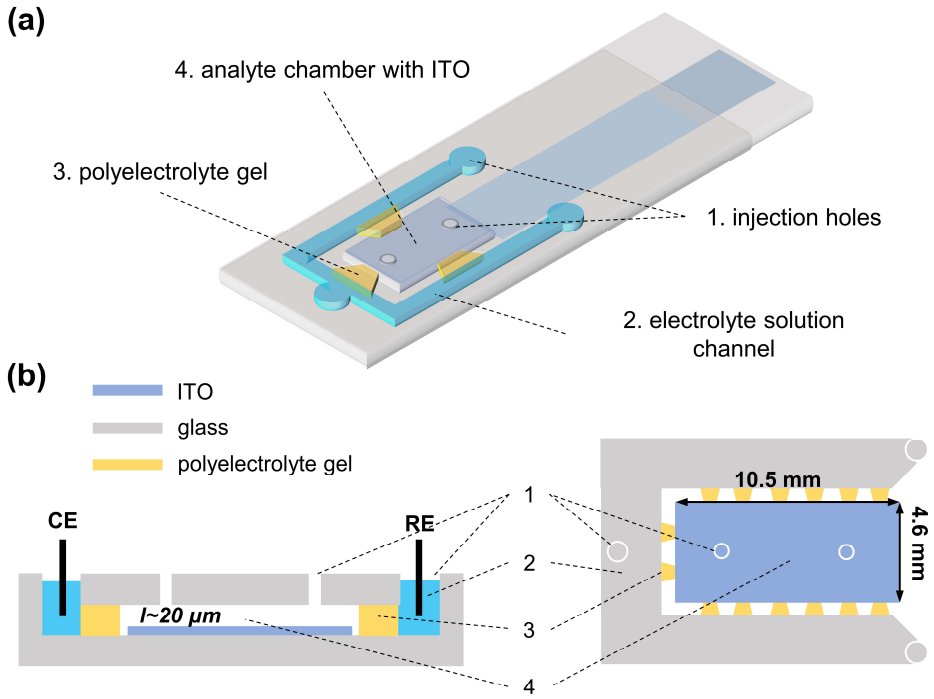

SCHEME 2. Synthesis of lipophilic polyelectrolyte salt bridge pLA-TFPB.

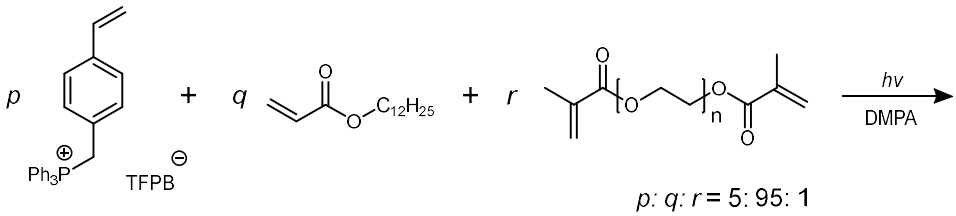

The validity of the TEAM as an electrochemical analytical device was investigated using the well-known redox species of ferrocyanide, *o*-tolidine, and ferrocene (Fc) (Figure 2). The cyclic voltammograms (CVs) of ferrocyanide exhibited very small peak-to-peak separations (ΔE_ps), ranging from 6 mV at a scan rate of 1 mV/s to 19 mV at a scan rate of 10 mV/s (Figure 2a and Table S1), as compared to 59 mV for a reversible one-electron transfer reaction under semi-infinite diffusion conditions. In addition, the current density (J) returned to the baseline after the peak potential, leading to symmetric peak shape. These characteristics are typical of thin-layer electrochemistry, as described above. As shown by the n–t plot for ferrocyanide oxidation (Figure 2b), n was measured accurately as 1. On the other hand, the n–t plot obtained in the TEAM without polyelectrolyte gel displayed constant increase of n due to the continuous influx of the reactants (Figure S3), indicating the necessity of the salt bridge to resolve the problematic lateral diffusion in conventional thin-layer cells. The feasibility of the TEAM was further demonstrated using *o*-tolidine, which undergoes quasi-reversible two-electron oxidation under acidic condition[36,37]. Likewise, a CV with a small ΔE_p was observed, and constant potential electrolysis resulted in n of *o*-tolidine oxidation as 2 (Figure 2c and 2d).

Finally, the compatibility of the TEAM with organic solutions was investigated with Fc in various organic solvents including acetonitrile (MeCN), acetone, dichloromethane (DCM), and tetrahydrofuran (THF) (Figure 2e and 2f). The large ΔE_ps in the resulting CVs originate from both the sluggish electron transfer kinetics at ITO (Figure S4) and higher resistances of the organic solutions and pLA-TFPB polyelectrolyte gel. To be noted, the total resistance of solution and gel between WE and RE was 148 Ω for 1 M KCl aqueous solution of pDADMAC gel but was 2084 Ω for 0.1 M TBAP acetone of pLA-TFPB gel. In addition, the variance in $E_{1/2}$ could be rationalized by the different reorganization energies of Fc/Fc^+ in various solvents.[38,39] Nevertheless, in all cases, n values of 1 were obtained.

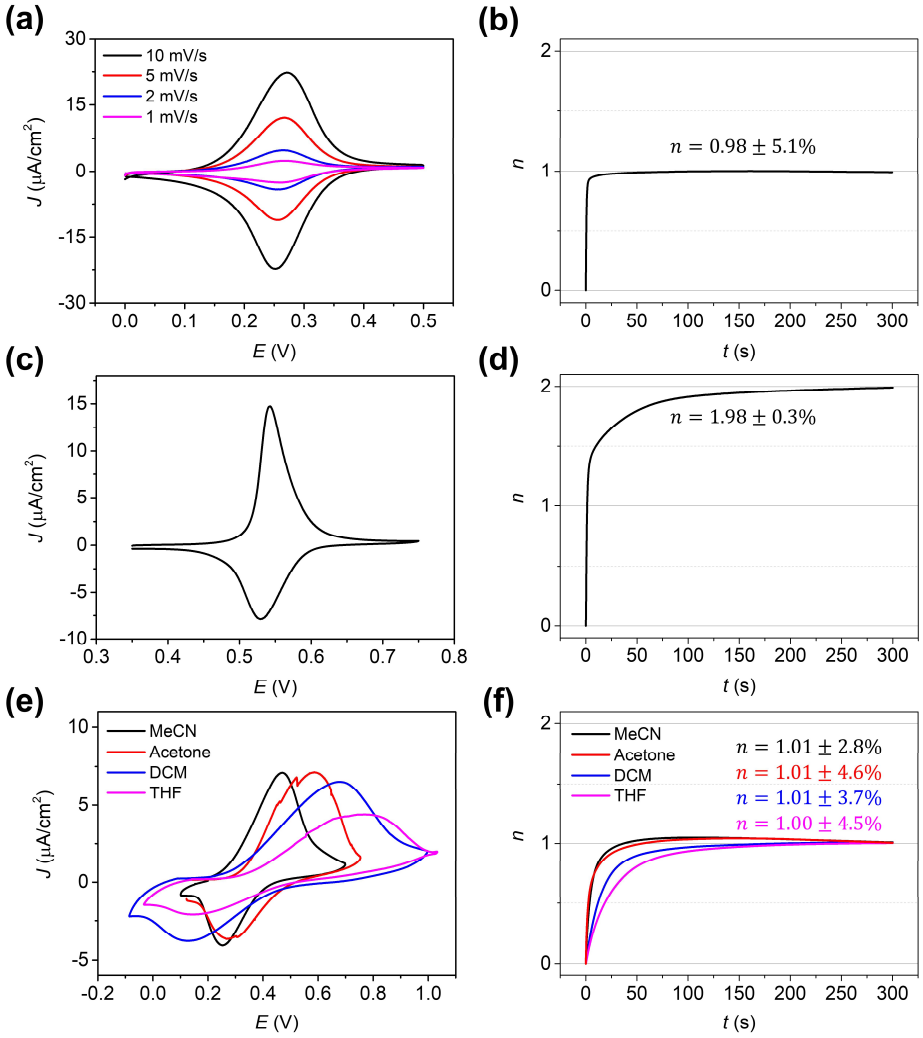

Figure 2. CVs and n–t plot of standard redox species using TEAM. (a, b) CVs and n–t plot (E_{app}=0.4 V) of 2 mM ferrocyanide in 1 M KCl. (c) CV (2 mV/s) and (d) n–t plot (E_{app}=0.7 V) of 1 mM *o*-tolidine in 0.2 M phosphate buffer (pH 2). (e) CVs (10 mV/s) and (f) n–t plot of 1 mM ferrocene in 0.1 M $TBAPF_6$ MeCN (E_{app}=0.5 V), acetone (E_{app}=0.5 V), DCM (E_{app}=0.7 V), and THF (E_{app}=0. 7 V) solution.

Electrochemical study of FM 1-43 dye and spectroelectrochemical measurements. One of the areas that demands knowledge of oxidation potentials or n of a molecule is neuroelectrochemistry because it is essential for amperometric detection of exocytosis events and quantitative analysis of released molecules from the measured current.[5,40] Exocytosis is mostly studied using either fluorescence microscopy or amperometry. As these two techniques provide complementary information, combining the two with an electroactive fluorescent dye provides coupled information with both high spatial and temporal resolutions.[41,42] FM 1-43, a fluorescent styryl dye widely used for visualizing exocytosis by entering or exiting synaptic vesicles,[43] can be utilized as such dual-functional fluorescent and electrochemical probe for monitoring exocytosis (Figure 3a). For such purpose, investigations of electrochemical activity and n of FM 1-43 are essential. The CV of FM 1-43 at ITO

electrode in semi-infinite diffusion condition proves the electroactivity of FM 1-43 (Figure 3a), but still lacks the information of *n* to enable quantitative analysis of exocytosis events and its correlation between electrochemical activity and optical properties.

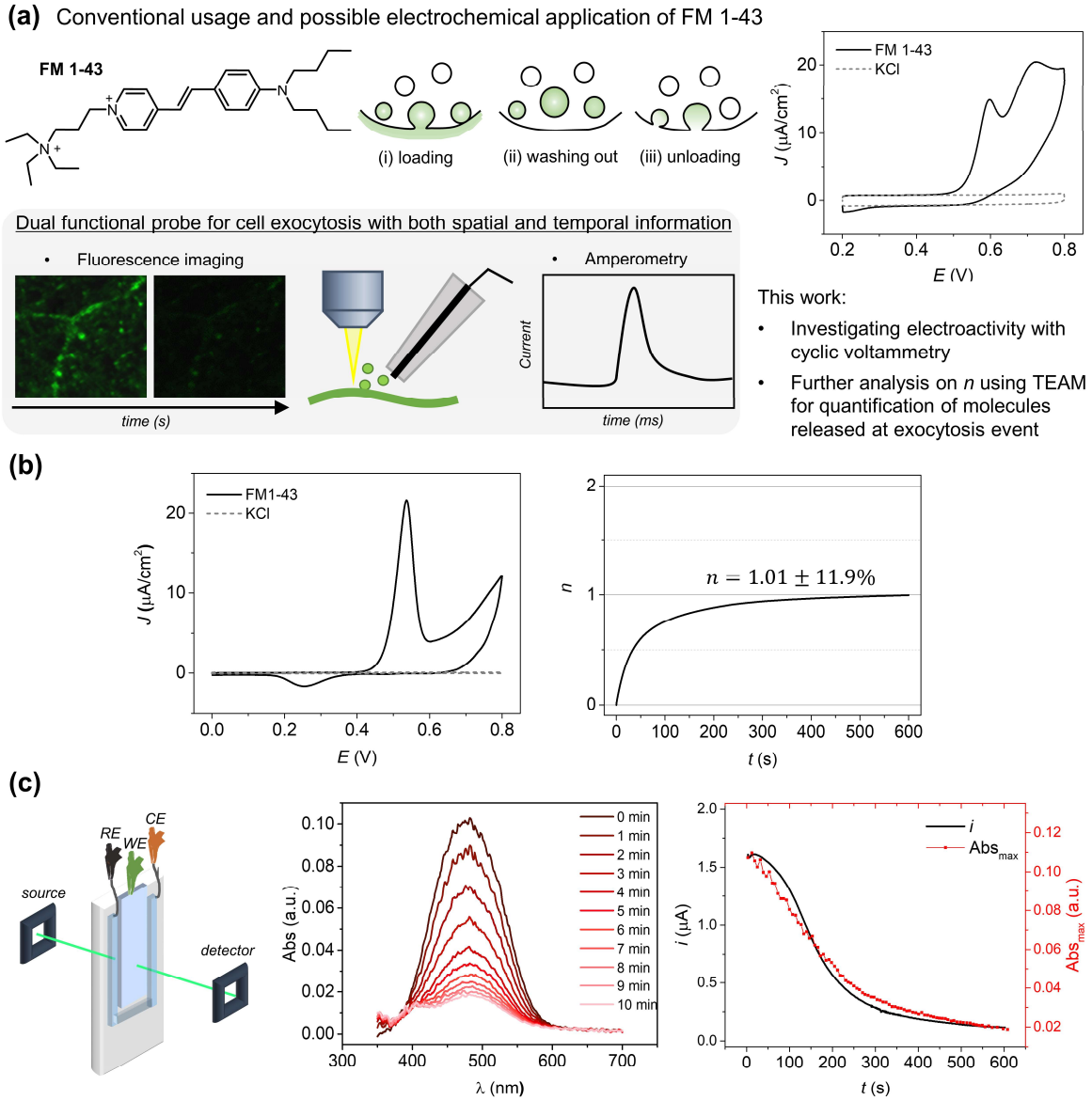

Figure 3. Electrochemical study of FM1-43: its background and significance. (a) Depiction of conventional use of FM 1-43 as fluorescent exocytosis probe in neurochemistry and CV of 50 μM FM 1-43 in 0.1 M KCl on ITO (50 mV/s). Scheme (second row) illustrates the proposed application of FM 1-43 as an electroactive fluorescent dual-functional probe of exocytosis. (b) CV (5mV/s) and *n*–*t* plot (E_{app}=0.5 V) of 2.5 mM FM 1-43 in 1 M KCl using TEAM. (c) Scheme of spectroelectrochemistry setup using TEAM (left). UV-VIS absorption spectra of 2.5 mM FM 1-43 in 1M KCl obtained with simultaneous electrolysis at 0.5 V (middle), and co-plot of the maximum absorbance with current measured *in situ* (right).

To further address the issues above, FM 1-43 was analyzed using the TEAM (Figure 3b). The CV exhibited a sharp anodic peak with E_p of 0.54 V followed by a broad anodic current, with better-defined peaks than CV under semi-infinite diffusion condition. The *n* value determined for the first oxidation step was 1, suggesting the stoichiometry to count the number of FM 1-43 molecules from the amperometric peak at 0.5 V during exocytosis. Considering the high electron density of p-orbital of the nitrogen atom in a conjugated system, the first oxidation is expected to come from the tertiary nitrogen.[44,45] It is also in consensus with the reports that the cyanine dye loses one electron to form a radical dication suggested by Lenhard *et al*.[46] Next, the spectroscopic change of FM 1-43 upon electrochemical reaction was investigated (Figure 3c). Because of the transparency

of the ITO electrode, the TEAM could be used as an *in situ* spectroelectrochemical cell with a path length of 20 μm, which may be favorable for minimizing the interruption from background signals or for investigating individual events in multi-step electrode reactions. The absorption spectra of FM 1-43 showed maximum absorption peak at 480 nm gradually decreasing with electrolysis at 0.5 V. It almost disappeared after complete electrolysis of 600 s, indicating the conjugation breakage induced by one-electron oxidation. The decrease in the maximum absorbance with time was consistent with the trend observed for the current measured simultaneously, exemplifying the real-time monitoring of spectroelectrochemical properties. The extinction of absorption wave upon oxidation is advantageous for an exocytosis probe in that the oxidized FM 1-43s would no longer affect the fluorescence signal.

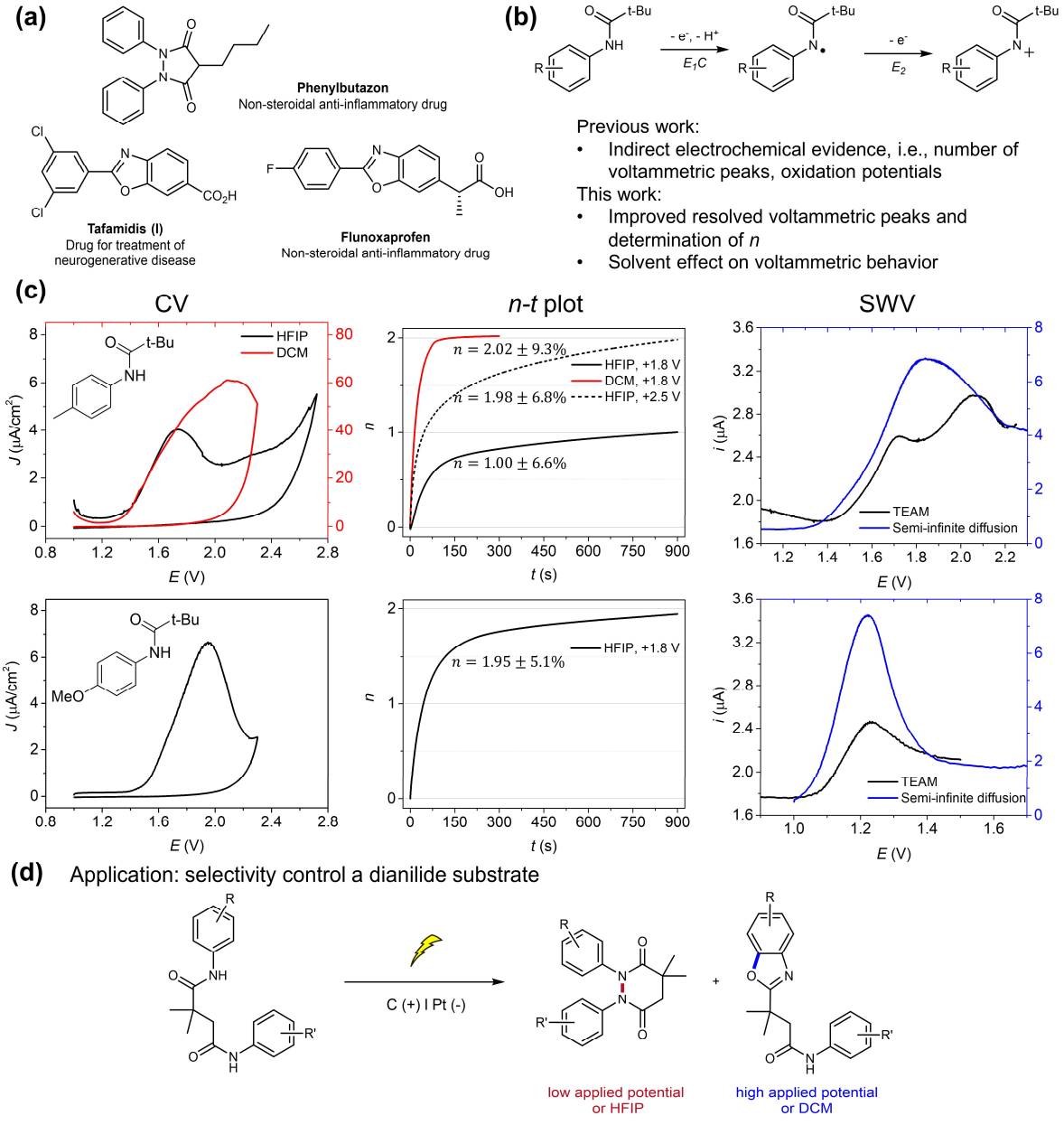

Figure 4. Electrochemical study of anilides: its background and significance. (a) Pharmaceuticals based on the structural motifs of pyrazolidine-3,5-diones and benzoxazoles. (b) Suggested electrochemical oxidation mechanism in the previous work and its limitations. (c) Electrochemical oxidation study of anilides using TEAM: CVs (10 mV/s) and *n–t* plots (E_{app}=1.8 and 2.5 V) of 1 mM 4-MePhNHPiv (1st-row) in 0.1 M $TBAPF_6$ of HFIP and DCM solution, and SWVs with TEAM or semi-infinite diffusion condition of 1 mM 4-MePhNHPiv (1st-row) in DCM. CV (10 mV/s), *n–t* plot (E_{app}=1.8 V), and SWVs with TEAM or semi-infinite diffusion condition of 1 mM 4-MeOPhNHPiv (2nd-row) in 0.1 M $TBAPF_6$ of HFIP solution. (d) Proposed application from the implication of this work: selectivity control a dianilide substrate to N-N bond or C-O bond formation by applied potential and choice of solvents.

Electrochemical study of pivanilides (*N*-centered electrochemistry). Anilide, an important building block molecule to produce pyrazolidine-3,5-diones and benzoxazoles which are important heterocyclic motifs appearing in natural products and drugs,[47–52] provides a key ring skeleton for many other medicinally relevant compounds (Figure 4a).[53–57] One of the simple routes to these compounds was previously reported to be the electrochemical N-N bond formation of dianilide by anodic oxidation of anilide.[58] The electrochemical oxidation pathway in hexafluoroisopropanol (HFIP) solvent was suggested as an *ECE* mechanism (Figure 4b): subsequent single electron transfer (SET) and deprotonation to amidyl radical followed by another SET to cation. It was supported by evidences including the number of peaks and oxidation potentials in the voltammograms and product analysis from electrosynthesis of dianilide via N–N bond formation. However, the number of voltammetric peaks alone is insufficient to support the mechanism due to lack of quantitative information in electrochemical analysis.

As accurate measurements of *n* and distinguishable voltammetric peaks can provide a better understanding of the oxidation mechanism, electroanalyses were performed using the TEAM (Figure 4c and Figure S5). The voltammogram of *N*-(*p*-tolyl)pivalamide (4-MePhNHPiv) exhibited two distinct peaks in hexafluoroisopropanol (HFIP), with each peak corresponding to single-electron transfer (SET), in agreement with the previously suggested mechanism.[58] For an anilide with a more electron-donating substituent, *N*-(4-methoxyphenyl)pivalamide (4-MeOPhNHPiv), a voltammogram with a single peak was obtained, corresponding to two-electron transfer. Interestingly, the voltammogram of 4-MePhNHPiv in DCM showed a single peak corresponding to two-electron transfer. These observations were further confirmed by the SWV for both anilides. Owing to the superior resolution of SWV in the TEAM, two distinct peaks were obtained for 4-MePhNHPiv in DCM with a voltage difference of approximately 300 mV, whereas a single peak was observed under semi-infinite diffusion conditions. The overlap of the two oxidation potentials is presumably ascribable to poor stabilization of the radical intermediate by the solvent, which would promote facile two-electron transfer. Furthermore, in both CV and SWV measurements, the two oxidation peaks for 4-MeOPhNHPiv in HFIP overlapped because the cation formed during the second oxidation process could be stabilized by resonance, similar to quinone imine-like structures.[58]

We further envision the opportunity of selectivity control of a dianilide substrate (Figure 4d). By constant potential electrolysis at the earlier voltammetric peak regime, radical pathway by SET would be predominant, leading to selective electrochemical N-N bond formation. On the other hand, cationic pathway may be predominant by higher applied potential of a later voltammetric peak, producing C-O bond. In the case of the anilide with single voltammetric peak of two-electron transfer, electrochemical C-O bond will be specifically produced. The choice of solvent will also influence the reaction, as indicated by the change of the shape of voltammograms of anilide upon solvent.

Electrochemical study of alkyltrifluoroborate salt (C(sp^3)-centered electrochemistry). The versatility of organoboranes provides access to valuable transformations in many fields of organic synthesis, pharmaceuticals, and materials science,[59–64] with recent attention focused on photoelectrochemical[60] and electrochemical reactions (Figure 5a).[59,64,65] Boronate complex or alkyltrifluoroborate salt have negative charge (polarity) analogous to organolithium or Grignard reagents, thereby active for the oxidation of carbon-centered electrochemistry.[61,65] Inagi *et al.* investigated the electrochemical oxidation of organoboranes including alkyltrifluoroborate salt in terms of oxidation potentials and studied one-electron oxidation using voltammetric analysis and DFT calculations.[59,63] For synthesis, the electrochemical generation of carbocations, implying two-electron transfer, has been recognized for a few examples.[59,65] However, the second oxidation process has not been characterized by electrochemical methods.

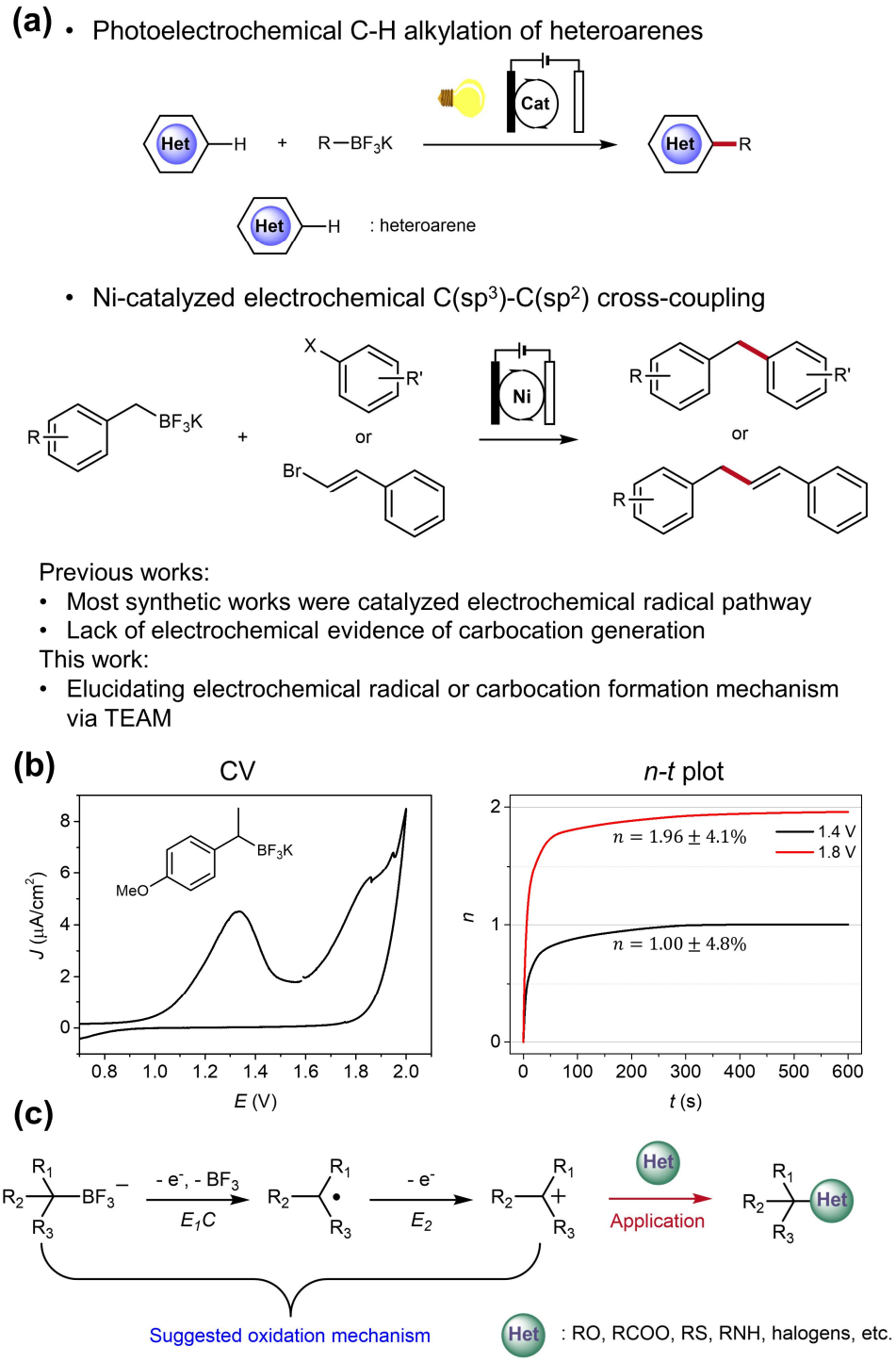

Figure 5. Electrochemical study of alkyltrifluoroborate salt: its background and significance. (a) Previous synthetic strategies using alkyltrifluoroborate salts. (b) Electrochemical oxidation study using TEAM from CV (10 mV/s) and *n*–*t* plots (E_{app}=1.4 and 1.8 V) of 1 mM (4-MeOPh)$CHCH_3BF_3K$ in 0.1 M $TBAPF_6$ of MeCN solution. (c) Suggested electrochemical oxidation mechanism based on this work and proposed application of the reaction scope of electrosynthesis producing carbon-heteroatom bonds via carbocation pathway.

Using TEAM, the electrochemistry of an alkyltrifluoroborate salt, trifluoro(1-(4-methoxyphenyl)-ethyl)-λ^4-borane potassium salt ((4-MeOPh)$CHCH_3BF_3K$), was studied (Figure 5b). The voltammogram showed two distinct peaks, each corresponding to SET, with a ΔE value of approximately 500 mV. The SET at 1.4 V is consistent with the well-known mechanism for (photo)electrochemical radical generation.[60,64,65] Moreover, the determination of an *n* value of 2 at 1.8 V implies that the carbocation pathway could be enabled by manipulating the applied potentials. Thus, the electrochemical oxidation

mechanism of the alkyltrifluoroborate salt may be suggested as an *ECE* mechanism (Figure 5c). As an application, electrochemical formation of carbon-heteroatom bonds by carbocation pathway is demonstrated in our recent work.[66]

CONCLUSION

In summary, we rediscovered thin-layer electrochemistry to develop a chip-type device, the TEAM, to clarify electrochemical reaction mechanisms. The thin-layer cell improved the resolution of the voltammetric peaks as compared to those obtained under semi-infinite diffusion conditions, as demonstrated by simulations and experiments. Notably, rapid and accurate determination of n with microliter-scale analytical volume was feasible. The introduction of a polyelectrolyte gel enabled bulk electrolysis with a minimal error by preventing lateral diffusion, regardless of the sluggish kinetics or complexity of the reactions. Using TEAM, voltammetric/coulometric analyses and spectroelectrochemical studies were successfully conducted on not only well-known redox species but also on organic compounds that require mechanistic study, as summarized in Table S2. This work reveals the potential of the TEAM as a compact and easy-to-use device for exploring electron transfer steps in the fields of electroorganic/organometallic chemistry. We believe that TEAM can contribute to organic electrosynthesis to gain insights for rational synthetic design without multistep screening or product analysis. Further developments will enable more complicated analyses of electrochemical reactions, such as investigating coupled chemical reactions or spectroelectrochemical detection of short-lived intermediates of electrochemical reactions.

EXPERIMENTAL SECTION

Chemicals

Potassium hexacyanoferrate(II) trihydrate (Ferrocyanide, 99%) , ferrocene (Fc, 98%), potassium chloride (KCl, ≥99.0%), tetrabutylammonium hexafluorophosphate ($TBAPF_6$, 98%), tetrabutylammonium perchlorate (TBAP, ≥99.0%), 3-(Trimethoxysilyl)propyl methacrylate (TMSMA, ≥97.0%), acetic acid, diallyldimethylammonium chloride solution (65 wt.% in H_2O), lithium phenyl-2,4,6-trimethylbenzoylphosphinate (LAP), *N,N'*-methylenebis(acrylamide), poly(ethylene glycol)dimethacylate (pEGMDA, average M_n 550), lauryl acrylate (90%), sodium tetrakis[3,5-bis(trifluoromethyl)phenyl]borate, triphenylphosphate (NaTFPB), 4-chloro α-methylstyrene, 2,2-Dimethoxy-2-phenylacetophenone (DMPA), methanol (anhydrous), and petroleum ether were purchased from Sigma-Aldrich. Sulfuric acid (95%, Daejung), hydrogen peroxide (H_2O_2, Samchun), ammonium hydroxide (NH_4OH, Daejung), *o*-tolidine (95%, Samchun), FM 1-43 (thermofisher), dichloromethane (DCM, 99%, Daejung), hexafluoroisopropanol (HFIP, 99%, Tokyo Chemical Industry), acetone (99%, Daejung), ethanol (99.5%, Daejung), tetrahydrofuran (THF, 99.9%, Riedel-de Haën), and acetonitrile (MeCN, 99%, Daejung) were purchased and all chemicals were used as received.

The pivanilides were synthesized by following the literature.[58,67] Note that all the pivanilides were recrystallized by petroleum ether prior to electrochemical characterization. The alkyltrifluoroborate salt of (4-MeOPh)$CHCH_3BF_3K$ was synthesized and details are described in Supporting Information. White solid of 51% yield; ^{1}H NMR (400 MHz, DMSO-d_6): δ = 6.95 (d, J = 8.2 Hz, 1H), 6.65 (d, J = 8.3 Hz, 1H), 3.66 (s, 2H), 1.50 (s, 1H), 1.00 (d, J = 7.2 Hz, 2H); ^{13}C NMR (101 MHz, DMSO-d_6): δ = 155.17, 144.28, 128.09, 112.43, 54.83, 17.79; ^{19}F NMR (376 MHz, DMSO-d_6): δ = -145.40; HRMS-ESI (m/z) $[M]^-$ calcd. for $C_9H_{11}BF_3O$, 203.08605; found: 203.0834.

Fabrication of chip

The TEAM was composed of indium tin oxide (ITO)-coated glass (30 Ω/cm^2, Omniscience, Korea) on one side and 20-μm etched slide glass (Marienfeld) on the other side. It was fabricated following procedures reported.[68] In short, ITO-coated glass was dried at 120° C and was spin-coated with HDMS then with photoresist (AZ4620, Clariant). The photoresist was patterned by UV exposure of 17 mJ/cm^2 for 16 s and development using AZ400K (AZ Electronic Materials). The ITO film was etched with Cu etchant (CE-100, Transene). At last, liftoff by sonication in acetone completed the patterned ITO glass. The glass was cleaned at piranha solution (sulfuric acid:H_2O_2=3:1) and patterned as the same above. The patterned glass was etched using buffered oxide etch 6:1 (Samchun) until the step height of 20 μm on average. After drilling the holes, the photoresist was removed with piranha solution. For bonding, the surface of the glasses was treated with ammonium water (NH_4OH: H2O: H_2O_2=2:2:1) for 1 h at 175 °C, then rinsed with distilled water to be thermally bonded in the furnace. The bonded chip was held at a temperature of 300 °C for one hour under a forming gas atmosphere (95% N_2 and 5% H_2) in a quartz tube furnace.

Forming polyelectrolyte gel salt bridge

For an aqueous solution compatible TEAM, poly(diallyldimethylammonium chloride) (pDADMAC) was employed as the salt bridge gel. The chip was pretreated with TMSMA solution (TMSMA:acetic acid:methanol=1:1:20) for 30 min in ambient condition. After being washed with methanol and water, it was filled with DADMAC monomer solution composed of 65% DADMAC solution added with 1% LAP as the photoinitiator and 1% *N, N'*-methylenebis(acrylamide) as the cross-linker. The chip was finally exposed to UV of 17 mJ/cm^2 for 1.2 s through a photomask to induce photopolymerization. For an organic solution compatible electrolysis chip, lauryl acrylate with monomer **1** was polymerized with pEGDMA as a crosslinker and DMPA as the photoinitiator to form the salt bridge gel. Monomer **1** was synthesized from the reaction of triphenylphosphine with 4-chloromethylstyrene, followed by anion exchange with NaTFPB, as reported[35]. The precursor solution composed of monomer **1**:lauryl acrylate:pEGDMA:DMPA with the ratio of 5:95:1:2, was injected into the chip. The salt bridge was

photopolymerized with exposure to UV for 16 s and successfully worked as a salt bridge in organic solvents of DCM, MeCN, THF, acetone, and HFIP.

The resistivity of polyelectrolyte gels was measured by electrochemical impedance spectroscopy (EIS) with potentiostat (Gamry Instruments). Nyquist plots were obtained in TEAM with DC voltage of open-circuit voltage and AC voltage of 5 mV in the frequency range from 100 kHz to 0.1 Hz. The solution and gel resistance was extracted from the *x*-intercept of the hemicircle of the Nyquist plot with ZSimpWin 3.22 software.

Electrochemical measurements

All the electrochemical measurements were performed with CHI 660 and 750 potentiostat (CH Instruments, TX, U.S.A.). Three electrode system was used with Pt wire as the counter electrode and Ag/AgCl wire in 3 M NaCl as the reference electrode. Aqueous solutions were prepared in 1 M KCl electrolyte solution in distilled water, and all the organic solutions were prepared in either 0.1 M $TBAPF_6$ or TBAP electrolyte solution. When performing electrochemical measurements with TEAM, the channel was filled with a high concentration electrolyte solution for decent conductivity between the working electrode and the reference electrode. Chronoamperometry technique was used for electrolysis and data were integrated with CHI software. For *n* determination, the potential to be applied (E_{app}) was selected based on cyclic voltammogram. The potential was chosen near the redox peak potential while no subsequent reactions would occur. E_{app} was applied for a few minutes until the slope of charge was the same as that of the blank solution. The constant charge after blank subtraction was substituted in Faraday's law of electrolysis, $Q = nFC^0V$, to calculate *n*, where Q is the charge, F is Faraday's constant, C^0 is concentration, and V is solution volume. The number of experiments was 5 for all the *n–t* plots obtained. For square wave voltammetry, step potential of 1 mV, amplitude of 15 mV, and frequency of 15 Hz was used if not stated otherwise. A microchip without polyelectrolyte gel was used for square wave voltammetry to enable clearer peak separation.

Note that the electrochemical activity of ITO for TEAM is sometimes inconsistent upon usage. The recovery step is often needed following the modified procedure: applying -1.0 V for 60 s in 1:10 (v:v) MeOH-H_2O solution.[69]

Simulation model

Digital simulations were performed with COMSOL Multiphysics v5.4 (COMSOL, Inc., Burlington, MA). 'Electroanalysis' module with 1D geometry was used for the simplicity, where one point was designated as the electrode and the boundary length was 20 μm or $\sqrt{2Dt}$ for cases of thin-layer model or semi-infinite diffusion model respectively. Parameters of the simulation were randomly given from generally accepted values. The diffusion coefficient was set as 5×10^{-6} cm^2/s for all species, E_1^0 was 0.5 V, cathodic transfer coefficient α was 0.5, the heterogeneous rate constants k_1^0 and k_2^0 were 0.00015 cm/s and 0.0001 cm/s respectively. Step potential for SWV was 2 mV, the amplitude was 15 mV, and the frequency was 15 Hz unless mentioned otherwise. The initial concentration of the reactant was 1 mM and zero for other species.

The electron transfer kinetics was governed by the Bulter-Volmer equation,

$$i = \mathrm{FA}k^0\left(C_O(0,t)\exp\left(-\frac{\alpha F\eta}{RT}\right) - C_R(0,t)\exp(\frac{(1-\alpha)F\eta}{RT})\right)$$

in which A is electrode area and η is the overpotential.

Square wave potential waveform was given using Heaviside function and modulo operator based on the previous report.[70] Currents were extracted at the end of each pulse by post-processing using MATLAB (Mathworks Inc.). Forward current and backward current were derived from positive and negative pulse each, and the net current was obtained by subtracting the backward current from the forward current.

ASSOCIATED CONTENT

The Supporting Information is available free of charge online. Experimental details; additional simulation data and explanation; cross-sectional diagram of TEAM; synthetic scheme of pLA-TFPB, peak-to-peak separation of ferrocyanide CVs; *n–t* plot without polyelectrolyte gel; CVs of Fc, 4-MePhNHPiv, and (4-MeOPh)$CHCH_3BF_3K$ in semi-infinite diffusion condition; summary of oxidation potential and *n*. (PDF)

Video of simulated concentration profile change in thin-layer cell, where the red line represents specie R; blue line for O; green line for O'; (Video S1)

AUTHOR INFORMATION

Corresponding Author

* tdchung@snu.ac.kr

Author Contributions

‡These authors contributed equally.

Notes

The authors declare no competing financial interests.

ACKNOWLEDGMENT

This work was supported by the National Research Foundation of Korea(NRF) grant funded by the Korean government(MSIT) (No. 2021R1A5A1030054, 2017R1E1A1A01074236).

REFERENCES

(1) Hisatomi, T.; Domen, K. Reaction Systems for Solar Hydrogen Production via Water Splitting with Particulate Semiconductor Photocatalysts. *Nat. Catal.* **2019**, *2* (5), 387–399. DOI: 10.1038/s41929-019-0242-6.

(2) Nilges, P.; Schröder, U. Electrochemistry for Biofuel Generation: Production of Furans by Electrocatalytic Hydrogenation of Furfurals. *Energy Environ. Sci.* **2013**, *6* (10), 2925–2931. DOI: 10.1039/c3ee41857j.

(3) Chadderdon, X. H.; Chadderdon, D. J.; Matthiesen, J. E.; Qiu, Y.; Carraher, J. M.; Tessonnier, J. P.; Li, W. Mechanisms of Furfural Reduction on Metal Electrodes: Distinguishing Pathways for Selective Hydrogenation of Bioderived Oxygenates. *J. Am. Chem. Soc.* **2017**, *139* (40), 14120–14128. DOI: 10.1021/jacs.7b06331.

(4) Nielsen, D. U.; Hu, X. M.; Daasbjerg, K.; Skrydstrup, T. Chemically and Electrochemically Catalysed Conversion of CO2 to CO with Follow-up Utilization to Value-Added Chemicals. *Nat. Catal.* **2018**, *1* (4), 244–254. DOI: 10.1038/s41929-018-0051-3.

(5) Lemaître, F.; Guille Collignon, M.; Amatore, C. Recent Advances in Electrochemical Detection of Exocytosis. *Electrochim. Acta* **2014**, *140*, 457–466. DOI: 10.1016/j.electacta.2014.02.059.

(6) Morofuji, T.; Shimizu, A.; Yoshida, J. Metal- and Chemical-Oxidant-Free C-H/C-H Cross-Coupling of Aromatic Compounds: The Use of Radical-Cation Pools. *Angew. Chem. Int. Ed.* **2012**, *51* (29), 7259–7262. DOI: 10.1002/anie.201202788.

(7) Morofuji, T.; Shimizu, A.; Yoshida, J. Heterocyclization Approach for Electrooxidative Coupling of Functional Primary Alkylamines with Aromatics. *J. Am. Chem. Soc.* **2015**, *137* (31), 9816–9819. DOI: 10.1021/jacs.5b06526.

(8) Waldvogel, S. R.; Mohle, S. Versatile Electrochemical C-H Amination via Zincke Intermediates. *Angew. Chem. Int. Ed.* **2015**, *54* (22), 6398–6399. DOI: 10.1002/anie.201502638.

(9) Horn, E. J.; Rosen, B. R.; Chen, Y.; Tang, J.; Chen, K.; Eastgate, M. D.; Baran, P. S. Scalable and Sustainable Electrochemical Allylic C-H Oxidation. *Nature* **2016**, *533* (7601), 77–81. DOI: 10.1038/nature17431.

(10) Fu, N.; Sauer, G. S.; Saha, A.; Loo, A.; Lin, S. Metal-Catalyzed Electrochemical Diazidation of Alkenes. *Science (80).* **2017**, *357* (6351), 575–579. DOI: 10.1126/science.aan6206.

(11) Kawamata, Y.; Yan, M.; Liu, Z.; Bao, D. H.; Chen, J.; Starr, J. T.; Baran, P. S. Scalable, Electrochemical Oxidation of Unactivated C-H Bonds. *J. Am. Chem. Soc.* **2017**, *139* (22), 7448–7451. DOI: 10.1021/jacs.7b03539.

(12) Costentin, C.; Savéant, J. M. Concepts and Tools for Mechanism and Selectivity Analysis in Synthetic Organic Electrochemistry. *Proc. Natl. Acad. Sci. U. S. A.* **2019**, *166* (23), 11147–11152. DOI: 10.1073/pnas.1904439116.

(13) Sandford, C.; Edwards, M. A.; Klunder, K. J.; Hickey, D. P.; Li, M.; Barman, K.; Sigman, M. S.; White, H. S.; Minteer, S. D. A Synthetic Chemist's Guide to Electroanalytical Tools for Studying Reaction Mechanisms. *Chem. Sci.* **2019**, *10* (26), 6404–6422. DOI: 10.1039/c9sc01545k.

(14) Hu, P.; Peters, B. K.; Malapit, C. A.; Vantourout, J. C.; Wang, P.; Li, J.; Mele, L.; Echeverria, P.-G.; Minteer, S. D.; Baran, P. S. Electroreductive Olefin–Ketone Coupling. *J. Am. Chem. Soc.* **2020**, *142* (50), 20979–20986. DOI: 10.1021/jacs.0c11214.

(15) Wang, H.; Liang, K.; Xiong, W.; Samanta, S.; Li, W.; Lei, A. Electrochemical Oxidation-Induced Etherification via C(Sp3)-H/O-H Cross-Coupling. *Sci. Adv.* **2020**, *6* (20), eaaz0590. DOI: 10.1126/sciadv.aaz0590.

(16) Siu, J. C.; Parry, J. B.; Lin, S. Aminoxyl-Catalyzed Electrochemical Diazidation of Alkenes Mediated by a Metastable Charge-Transfer Complex. *J. Am. Chem. Soc.* **2019**, *141* (7), 2825–2831. DOI: 10.1021/jacs.8b13192.

(17) Gnaim, S.; Takahira, Y.; Wilke, H. R.; Yao, Z.; Li, J.; Delbrayelle, D.; Echeverria, P. G.; Vantourout, J. C.; Baran, P. S. Electrochemically

Driven Desaturation of Carbonyl Compounds. *Nat. Chem.* **2021**, *13* (4), 367–372. DOI: 10.1038/s41557-021-00640-2.
(18) Song, L.; Fu, N.; Ernst, B. G.; Lee, W. H.; Frederick, M. O.; DiStasio, R. A.; Lin, S. Dual Electrocatalysis Enables Enantioselective Hydrocyanation of Conjugated Alkenes. *Nat. Chem.* **2020**, *12* (8), 747–754. DOI: 10.1038/s41557-020-0469-5.
(19) Saveant, J. M. Molecular Electrochemistry: Recent Trends and Upcoming Challenges. *ChemElectroChem* **2016**, *3* (12), 1967–1977. DOI: 10.1002/celc.201600430.
(20) Wise, C. F.; Agarwal, R. G.; Mayer, J. M. Determining Proton-Coupled Standard Potentials and X-H Bond Dissociation Free Energies in Nonaqueous Solvents Using Open-Circuit Potential Measurements. *J. Am. Chem. Soc.* **2020**, *142* (24), 10681–10691. DOI: 10.1021/jacs.0c01032.
(21) Peters, B. K.; Rodriguez, K. X.; Reisberg, S. H.; Beil, S. B.; Hickey, D. P.; Kawamata, Y.; Collins, M.; Starr, J.; Chen, L.; Udyavara, S.; Klunder, K.; Gorey, T. J.; Anderson, S. L.; Neurock, M.; Minteer, S. D.; Baran, P. S. Scalable and Safe Synthetic Organic Electroreduction Inspired by Li-Ion Battery Chemistry. *Science.* **2019**, *363* (6429), 838–845. DOI: 10.1126/science.aav5606.
(22) Mouahid, O. El; Coutanceau, C.; Belgsir, E. M.; Crouigneau, P.; Léger, J. M.; Lamy, C. Electrocatalytic Reduction of Dioxygen at Macrocycle Conducting Polymer Electrodes in Acid Media. *J. Electroanal. Chem.* **1997**, *426* (1–2), 117–123. DOI: 10.1016/s0022-0728(96)04980-7.
(23) Zhou, R.; Zheng, Y.; Jaroniec, M.; Qiao, S. Z. Determination of the Electron Transfer Number for the Oxygen Reduction Reaction: From Theory to Experiment. *ACS Catal.* **2016**, *6* (7), 4720–4728. DOI: 10.1021/acscatal.6b01581.
(24) Baranski, A. S.; Fawcett, W. R.; Gilbert, C. M. Use of Microelectrodes for the Rapid Determination of the Number of Electrons Involved in an Electrode Reaction. *Anal. Chem.* **1985**, *57* (1), 166–170. DOI: 10.1021/ac00279a041.
(25) Nishiumi, T.; Abdul, M. M.; Aoki, K. Determination of the Number of Electrons by Chronoamperometry at Small Electrodes. *Electrochem. Commun.* **2005**, *7* (12), 1213–1217. DOI: 10.1016/j.elecom.2005.08.030.
(26) Treimer, S.; Tang, A.; Johnson, D. C. A Consideration of the Application of Koutecký-Levich Plots in the Diagnoses of Charge-Transfer Mechanisms at Rotated Disk Electrodes. *Electroanalysis* **2002**, *14* (3), 165–171. DOI: 10.1002/1521-4109(200202)14:3<165::AID-ELAN165>3.0.CO;2-6.
(27) Hubbard, A. T. Study of the Kinetics of Electrochemical Reactions by Thin-Layer Voltammetry. *J. Electroanal. Chem.* **1969**, *22* (2), 165–174. DOI: 10.1016/s0022-0728(71)80210-3.
(28) Christensen, C. R.; Anson, F. C. Application of Thin Layer Chronopotentiometry to Kinetic Studies. *Anal. Chem.* **1964**, *36* (3), 495–497. DOI: 10.1021/ac60209a052.
(29) Oglesby, D. M.; Omang, S. H.; Reilley, C. N. Thin Layer Electrochemical Studies Using Controlled Potential or Controlled Current. *Anal. Chem.* **1965**, *37* (11), 1312–1316. DOI: 10.1021/ac60230a007.
(30) McClure, J. E.; Maricle, D. L. A New Dip-Type Thin-Layer Electrolysis Cell. n-Value Determinations in Non-Aqueous Systems. *Anal. Chem.* **1967**, *39* (2), 236–238. DOI: 10.1021/ac60246a010.
(31) Murray, R. W.; Heineman, W. R.; O'Dom, G. W. An Optically Transparent Thin Layer Electrochemical Cell. *Anal. Chem.* **1967**, *39* (13), 1666–1668. DOI: 10.1021/ac50156a052.
(32) Gamage, R. S. K. A.; Umapathy, S.; McQuillan, A. J. OTTLE Cell Study of the UV-Visible and FTIR Spectroelectrochemistry of the Radical Anion and Dianion of 1,4-Benzoquinone in DMSO Solutions. *J. Electroanal. Chem.* **1990**, *284* (1), 229–235. DOI: 10.1016/0022-0728(90)87075-U.
(33) Kim, S. K.; Lim, H.; Chung, T. D.; Kim, H. C. A Miniaturized Electrochemical System with a Novel Polyelectrolyte Reference Electrode and Its Application to Thin Layer Electroanalysis. *Sens. Actuators B* **2006**, *115* (1), 212–219. DOI: 10.1016/j.snb.2005.09.005.
(34) Ono, T.; Sugimoto, T.; Shinkai, S.; Sada, K. Lipophilic Polyelectrolyte Gels as Super-Absorbent Polymers for Nonpolar Organic Solvents. *Nat. Mater.* **2007**, *6* (6), 429–433. DOI: 10.1038/nmat1904.
(35) Sunaga, S.; Kokado, K.; Sada, K. Lipophilic Polyelectrolyte Gel Derived from Phosphonium Borate Can Absorb a Wide Range of Organic Solvents. *Soft Matter* **2018**, *14* (4), 581–585. DOI: 10.1039/c7sm01841j.
(36) Deangelis, T. P.; Heineman, W. R. An Electrochemical Experiment Using an Optically Transparent Thin Layer Electrode. *J. Chem. Educ.* **1976**, *53* (9), 594–597. DOI: 10.1021/ed053p594.
(37) Yu, J. S.; Yang, C.; Fang, H. Q. Variable Thickness Thin-Layer Cell for Electrochemistry and in Situ UV- VIS Absorption, Luminescence and Surface-Enhanced Raman Spectroelectrochemistry. *Anal. Chim. Acta* **2000**, *420* (1), 45–55. DOI: 10.1016/S0003-2670(00)01005-9.
(38) Tsierkezos, N. G. Cyclic Voltammetric Studies of Ferrocene in Nonaqueous Solvents in the Temperature Range from 248.15 to 298.15 K. *J. Solution Chem.* **2007**, *36* (3), 289–302. DOI: 10.1007/s10953-006-9119-9.
(39) Tsierkezos, N. G.; Ritter, U. Electrochemical Impedance Spectroscopy and Cyclic Voltammetry of Ferrocene in Acetonitrile/Acetone System. *J. Appl. Electrochem.* **2010**, *40* (2), 409–417. DOI: 10.1007/s10800-009-0011-3.
(40) Mosharov, E. V. Analysis of Single-Vesicle Exocytotic Events Recorded by Amperometry. *Methods Mol. Biol.* **2008**, *440* (9), 315–327. DOI: 10.1007/978-1-59745-178-9_24.
(41) Liu, X.; Savy, A.; Maurin, S.; Grimaud, L.; Darchen, F.; Quinton, D.; Labbé, E.; Buriez, O.; Delacotte, J.; Lemaître, F.; Guille-Collignon, M. A Dual Functional Electroactive and Fluorescent Probe for Coupled Measurements of Vesicular Exocytosis with High Spatial and Temporal Resolution. *Angew. Chem. Int. Ed.* **2017**, *56* (9), 2366–2370. DOI: 10.1002/anie.201611145.
(42) Liu, X.; Hu, L.; Pan, N.; Grimaud, L.; Labbé, E.; Buriez, O.; Delacotte, J.; Lemaître, F.; Guille-Collignon, M. Coupling Electrochemistry and TIRF-Microscopy with the Fluorescent False Neurotransmitter FFN102 Supports the Fluorescence Signals during Single Vesicle Exocytosis Detection. *Biophys. Chem.* **2018**, *235,* 48–55. DOI: 10.1016/j.bpc.2018.02.004.
(43) Cochilla, A. J.; Angleson, J. K.; Betz, W. J. Monitoring Secretory Membrane With Fm1-43 Fluorescence. *Annu. Rev. Neurosci.* **2002**, *22* (1), 1–10. DOI: 10.1146/annurev.neuro.22.1.1.
(44) Blanchard, P.; Malacrida, C.; Cabanetos, C.; Roncali, J.; Ludwigs, S. Triphenylamine and Some of Its Derivatives as Versatile Building Blocks for Organic Electronic Applications. *Polym. Int.* **2019**, *68* (4), 589–606. DOI: 10.1002/pi.5695.
(45) Levitskiy, O. A.; Dulov, D. A.; Nikitin, O. M.; Bogdanov, A. V.; Eremin, D. B.; Paseshnichenko, K. A.; Magdesieva, T. V. Competitive Routes for Electrochemical Oxidation of Substituted Diarylamines: The Guidelines. *ChemElectroChem* **2018**, *5* (22), 3391–3410. DOI: /10.1002/celc.201801177.
(46) Lenhard, J. R.; Cameron, A. D. Electrochemistry and Electronic Spectra of Cyanine Dye Radicals in Acetonitrile. *J. Phys. Chem.* **1993**, *97* (19), 4916–4925. DOI: 10.1021/j100121a009.
(47) Kutterer, K. M. K.; Davis, J. M.; Singh, G.; Yang, Y.; Hu, W.; Severin, A.; Rasmussen, B. A.; Krishnamurthy, G.; Failli, A.; Katz, A. H. 4-

Alkyl and 4,4′-Dialkyl 1,2-Bis(4-Chlorophenyl)Pyrazolidine-3,5-Dione Derivatives as New Inhibitors of Bacterial Cell Wall Biosynthesis. *Bioorg. Med. Chem. Lett.* **2005**, *15* (10), 2527–2531. DOI: https://doi.org/10.1016/j.bmcl.2005.03.058.

(48) Gilbert, A. M.; Failli, A.; Shumsky, J.; Yang, Y.; Severin, A.; Singh, G.; Hu, W.; Keeney, D.; Petersen, P. J.; Katz, A. H. Pyrazolidine-3,5-Diones and 5-Hydroxy-1H-Pyrazol-3(2H)-Ones, Inhibitors of UDP-N-Acetylenolpyruvyl Glucosamine Reductase. *J. Med. Chem.* **2006**, *49* (20), 6027–6036. DOI: 10.1021/jm060499t.

(49) Deng, G.; Li, W.; Shen, J.; Jiang, H.; Chen, K.; Liu, H. Pyrazolidine-3,5-Dione Derivatives as Potent Non-Steroidal Agonists of Farnesoid X Receptor: Virtual Screening, Synthesis, and Biological Evaluation. *Bioorg. Med. Chem. Lett.* **2008**, *18* (20), 5497–5502. DOI: 10.1016/j.bmcl.2008.09.027.

(50) Nishiu, J.; Ito, M.; Ishida, Y.; Kakutani, M.; Shibata, T.; Matsushita, M.; Shindo, M. JTP-426467 Acts as a Selective Antagonist for Peroxisome Proliferator-Activated Receptor Γin Vitro and in Vivo. *Diabetes, Obes. Metab.* **2006**, *8* (5), 508–516. DOI: 10.1111/j.1463-1326.2005.00536.x.

(51) Zhang, X.-Y.; Gu, Y.-F.; Chen, T.; Yang, D.-X.; Wang, X.-X.; Jiang, B.-L.; Shao, K.-P.; Zhao, W.; Wang, C.; Wang, J.-W.; Zhang, Q.-R.; Liu, H.-M. Synthesis, in Vitro and in Vivo Anticancer Activities of Novel 4-Substituted 1,2-Bis(4-Chlorophenyl)-Pyrazolidine-3,5-Dione Derivatives. *Med. Chem. Comm.* **2015**, *6* (10), 1781–1786. DOI: 10.1039/C5MD00240K.

(52) Aiba *née* Kaneko, M.; Hirota, M.; Kouzuki, H.; Mori, M. Prediction of Genotoxic Potential of Cosmetic Ingredients by an *in Silico* Battery System Consisting of a Combination of an Expert Rule-Based System and a Statistics-Based System. *J. Toxicol. Sci.* **2015**, *40* (1), 77–98. DOI: 10.2131/jts.40.77.

(53) Bakthadoss, M.; Mushaf, M. A Distal Vinyl Shift (DVS) through Quadruple Domino Reaction: Synthesis of: N -Vinyl Benzoheterocyclic Scaffolds. *RSC Adv.* **2018**, *8* (22), 12152–12156. DOI: 10.1039/c8ra01478g.

(54) Ueki, M.; Ueno, K.; Shibata, K.; Oi, S.; Miyadoh, S.; Abe, K.; Taniguchi, M. UK-1, A Novel Cytotoxic Metabolite from Streptomyces SP. 517-02: I. Taxonomy, Fermentation, Isolation, Physico-Chemical and Biological Properties. *J. Antibiot.* **1993**, *46* (7), 1089–1094. DOI: 10.7164/antibiotics.46.1089.

(55) Leventhal, L.; Brandt, M. R.; Cummons, T. A.; Piesla, M. J.; Rogers, K. E.; Harris, H. A. An Estrogen Receptor-β Agonist Is Active in Models of Inflammatory and Chemical-Induced Pain. *Eur. J. Pharmacol.* **2006**, *553* (1), 146–148. DOI: 10.1016/j.ejphar.2006.09.033.

(56) Steinhilber, D.; Schubert-Zsilavecz, M.; Roth, H. J. *Medizinische Chemie*. **2005**, *36* (36). DOI: 10.1002/chin.200536214.

(57) Davidson, J. P.; Corey, E. J. First Enantiospecific Total Synthesis of the Antitubercular Marine Natural Product Pseudopteroxazole. Revision of Assigned Stereochemistry. *J. Am. Chem. Soc.* **2003**, *125* (44), 13486–13489. DOI: 10.1021/ja0378916.

(58) Gieshoff, T.; Kehl, A.; Schollmeyer, D.; Moeller, K. D.; Waldvogel, S. R. Insights into the Mechanism of Anodic N-N Bond Formation by Dehydrogenative Coupling. *J. Am. Chem. Soc.* **2017**, *139* (35), 12317–12324. DOI: 10.1021/jacs.7b07488.

(59) Suzuki, J.; Tanigawa, M.; Inagi, S.; Fuchigami, T. Electrochemical Oxidation of Organotrifluoroborate Compounds. *ChemElectroChem* **2016**, *3* (12), 2078–2083. DOI: 10.1002/celc.201600451.

(60) Yan, H.; Hou, Z. W.; Xu, H. C. Photoelectrochemical C−H Alkylation of Heteroarenes with Organotrifluoroborates. *Angew. Chem. Int. Ed.* **2019**, *58* (14), 4592–4595. DOI: 10.1002/anie.201814488.

(61) Kaur, P.; Khatik, G. L.; Nayak, S. K. A Review on Advances in Organoborane-Chemistry: Versatile Tool in Asymmetric Synthesis. *Curr. Org. Synth.* **2016**, *14* (5), 665–682. DOI: 10.2174/1570179414666161104162038.

(62) Fyfe, J. W. B.; Watson, A. J. B. Recent Developments in Organoboron Chemistry: Old Dogs, New Tricks. *Chem* **2017**, *3* (1), 31–55. DOI: 10.1016/j.chempr.2017.05.008.

(63) Inagi, S.; Fuchigami, T. Electrochemical Properties and Reactions of Organoboron Compounds. *Curr. Opin. Electrochem.* **2017**, *2* (1), 32–37. DOI: 10.1016/j.coelec.2017.02.007.

(64) Luo, J.; Hu, B.; Wu, W.; Hu, M.; Liu, T. L. Nickel-Catalyzed Electrochemical C(Sp3)−C(Sp2) Cross-Coupling Reactions of Benzyl Trifluoroborate and Organic Halides**. *Angew. Chem. Int. Ed.* **2021**, *60* (11), 6107–6116. DOI: 10.1002/anie.202014244.

(65) Inagi, S.; Fuchigami, T. Electrochemical Properties and Reactions of Organoboron Compounds. *Curr. Opin. Electrochem.* **2017**, *2* (1), 32–37. DOI: 10.1016/j.coelec.2017.02.007.

(66) Go, S. Y.; Chung, H.; Shin, S. J.; Ahn, S.; Youn, J. H.; Im, T. Y.; Kim, J. Y.; Chung, T. D.; Lee, H. G. A Unified Synthetic Strategy to Introduce Heteroatoms via Electrochemical Functionalization of Alkyl Organoboron Reagents. *ChemRxiv* **2021**. DOI: 10.33774/chemrxiv-2021-bvf1l.

(67) Mathew, B. P.; Yang, H. J.; Kim, J.; Lee, J. Bin; Kim, Y.-T.; Lee, S.; Lee, C. Y.; Choe, W.; Myung, K.; Park, J.-U.; Hong, S. Y. An Annulative Synthetic Strategy for Building Triphenylene Frameworks by Multiple C−H Bond Activations. *Angew. Chem. Int. Ed.* **2017**, *56* (18), 5007–5011. DOI: 10.1002/anie.201700405.

(68) Kang, C. M.; Joo, S.; Bae, J. H.; Kim, Y. R.; Kim, Y.; Chung, T. D. In-Channel Electrochemical Detection in the Middle of Microchannel under High Electric Field. *Anal. Chem.* **2012**, *84* (2), 901–907. DOI: 10.1021/ac2016322.

(69) Ribeiro, C. de L.; Santos, J. G. M.; de Souza, J. R.; Pereira-da-Silva, M. A.; Paterno, L. G. Electrochemical Oxidation of Salicylic Acid at ITO Substrates Modified with Layer-by-Layer Films of Carbon Nanotubes and Iron Oxide Nanoparticles. *J. Electroanal. Chem.* **2017**, *805* (15), 53–59. DOI: 10.1016/J.JELECHEM.2017.09.063.

(70) Dauphin-Ducharme, P.; Arroyo-Currás, N.; Kurnik, M.; Ortega, G.; Li, H.; Plaxco, K. W. Simulation-Based Approach to Determining Electron Transfer Rates Using Square-Wave Voltammetry. *Langmuir* **2017**, *33* (18), 4407–4413. DOI: 10.1021/acs.langmuir.7b00359.